Electronic Supplementary Information (ESI)

Ultrathin amorphous manganese dioxide nanosheets synthesized with controllable width

Chengjun Xu,*[,a] Shan Shi,[a,b] Yige Sun,[a] Yanyi Chen,[a] and Feiyu Kang[a,b]

Materials and Methods

1. Synthesis of two-dimentional MnO_2 nanosheets

The synthesis process of ultrathin MnO_2 nanosheet colloid is very simple and facile. $KMnO_4$ aqueous solution was firstly dispersed in isooctane and subsequently reduced by sodium bis(2-ethylhexyl) sulfosuccinate (Na(AOT)). Colloidal MnO_2 nanosheets were obtained by adding 0.1 mol L^{-1} (M) $KMnO_4$ aqueous solution in a 0.1 M Na(AOT)/isooctane, which was subjected to ultrasound for 30 minutes to yield a brown colloidal solution as shown in Figure S1a.

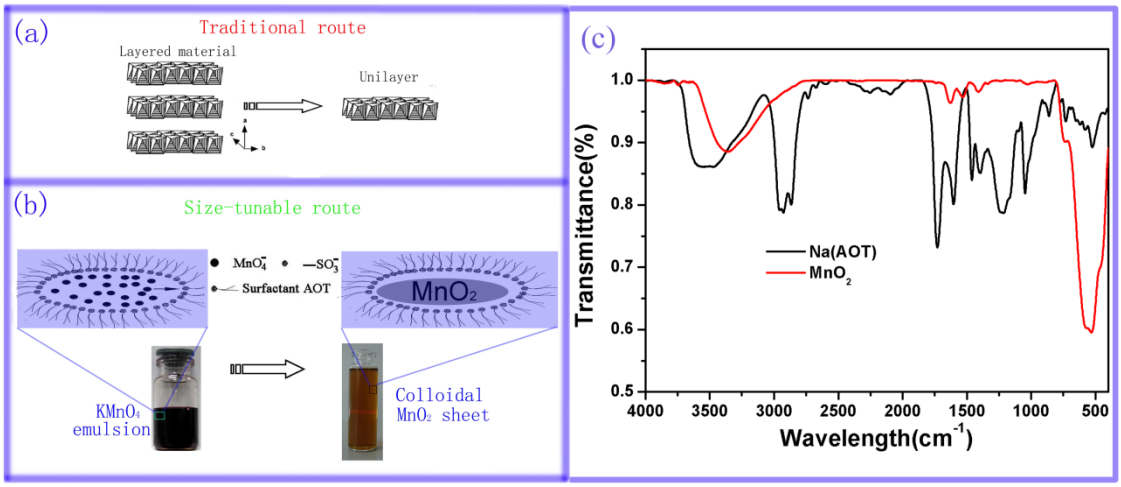

Fig S1 (a) Schematic of a traditional route to synthesize ultrathin MnO_2 nanosheets. These nanosheets are generally peeled off from a layered bulk material by a mechanical or chemical method without a size-tunable process. (b) Schematic of a size-tunable rout and photo images of emulsion and MnO_2 nanosheet colloidal. Right shows the Tyndall effect of the colloidal. This is one step process from emulsion to colloidal. (c) Fourier transformation infrared spectra (FTIR) of Na(AOT) and MnO_2 nanosheet

We controlled the water-surfactant molar ratio (W_0 = $[H_2O]/[AOT]$) values to synthesize various MnO_2 nanosheets. The W_0 values are ranging from 15, 22, 30, to 45, which are denoted as sample A, B, C, and D, respectively. The product was separated, washed copiously several times with distilled water and ethanol, and dried at 80 ℃ in vacuum for 12 h. FTIR spectra of Na(AOT) and MnO_2 nanosheet (sample C) are showed in Fig S1c. In the curve of MnO_2, the band at frequency 3370 cm^{-1} is representative of the O–H stretching vibration presented in the constitutional water. The bands observed in the low-frequency region ranging from 1000cm^{-1} to 400cm^{-1} reveal information about MnO_6 octahedral structure. The bands ranging from 1800cm^{-1} to 1000cm^{-1} in the curve of MnO_2

mainly represent the vibration due to interaction of Mn with surrounding species such as OH, O, and H. No characteristic peak of Na(AOT) are found in the curves of MnO_2, which indicates that the Na(AOT) are completely removed after washing process.

2. Synthesis of zero-dimentional MnO_2 nanosphere

100 mL 0.1 mol L^{-1} $KMnO_4$ and 0.15 mol L^{-1} $Mn(CH_3COO)_2$ aqueous solutions were prepared individually. 10 mL polyethylene glycol (PEG-400) was added in 100 mL $Mn(CH_3COO)_2$ solution, which has been stirred for 1 h. Then 100 mL 0.1 mol L^{-1} $KMnO_4$ aqueous solution was added quickly and stirred for 4 h at room temperature. The product was separated, washed copiously several times with distilled water and ethanol, and dried at 80 ℃ in vacuum for 12 h.

3. Synthesis of one-dimentional MnO_2 nanorod

Chemical co-precipitation technique was also used to be reference. 100 mL 0.1 mol L^{-1} $KMnO_4$ and 0.15 mol L^{-1} $Mn(CH_3COO)_2$ was quickly mixed and stirred for 4 h at room temperature. A dark brown precipitate was immediately obtained according to equation (1)

$$2Mn(\text{Ⅶ}) + 3Mn(\text{Ⅱ}) \rightarrow 5Mn(\text{Ⅳ}) \qquad (1)$$

The product was separated, washed copiously several times with distilled water, and dried at 80 ℃ in vacuum for 12 h.

Characterization

Powder X-ray diffraction (XRD) patterns of MnO_2 powders were obtained by using TW3040/60 diffractometer (Tanalygical Company, Holland) in which Cu-Kα was used as the source. Fourier transformation infrared spectra (FTIR) of the samples were measured from KBr sample pellets on a VERTEX 70 spectrometer. Morphology of MnO_2 was examined using transition electron microscope (Jeol JEM2100F), electron microscope (SEM, Hitachi, S-5200). The surface topography of the sample was visualized using atomic force microscopy (AFM, Shimadzu, SPM9600) instrument in tapping mode. X-ray photoelectron spectroscopy (XPS) studies were conducted with a VG Escalab 220i-XL instrument using X-rays magnesium anode (monochromatic K_α X-rays at 1253.6 eV) as a source. XPS spectra were analyzed and fitting using XPSPEAK software (version 4.1). Thermogravimetric analysis (TGA) and differential scanning calorimetry (DSC) for both samples were recorded in the temperature

range from ambient to 600 ℃ in nitrogen atmosphere at a heating rate of 10 ℃ per min using Sta449C (Netzsch) tester. The Raman sepctroscopy measurements have performed by Renishaw RM-1000 tester.

Electrochemical tests were performed with an Im6e (Zahner) electrochemical station. MnO_2 power was well-dispersed and drop coated on titanium substrate, which was further dried in vacuum at room temperature for 8 h. All electrodes with a loading mass of 0.25 ± 0.01 mg cm^{-2} were coated as the working electrode. The typical three-electrode assembly, in which a piece of platinum gauze and saturated calomel electrode were assembled as the counter and reference electrode, was employed.

All samples were subjected to cyclic voltammetric tests in 1 mol L^{-1} Na_2SO_4 solution. The potential range is from 0.0 to 0.8 V versus saturated calomel electrode (SCE) with sweep rates ranging from 2 to 100 mV s^{-1}. The specific capacitance (C) of electroactive material can be estimated using half the integrated area of the CV curve to obtain the charge (Q), and subsequently being divided the charge by the mass of the active material (m) and the width of the potential window (ΔV):

$$C = Q / \Delta V m \qquad (2)$$

1. MnO_2 nanosheets

SEM images of MnO_2 nanosheets

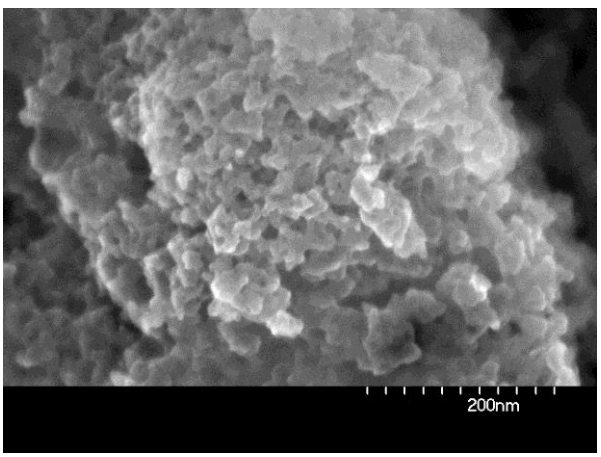

Fig. S2 SEM image of sample C

TEM images and AFM images of MnO_2 nanosheets

As is showed in Fig S3, both AFM and TEM images present sample C and sample D is ultrathin, with the average thickness of ca. 2 nm. Fig S3c' and Fig 3d' clearly indicate that the average widths of sample C and D are ca. 15 and 20 nm, respectively.

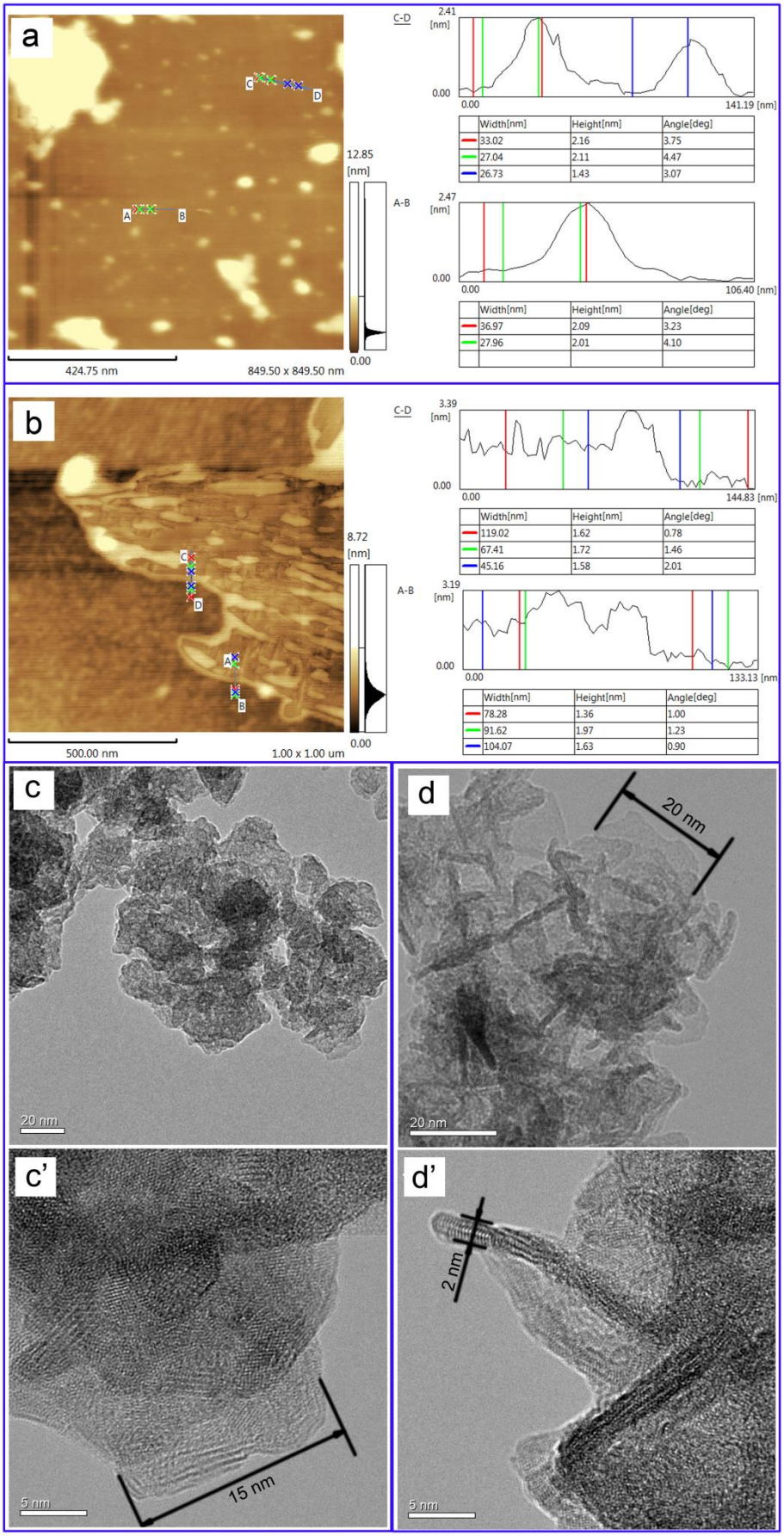

Fig. S3 AFM images of sample C (a) and sample D (b). Some cross-sectional analysis are also listed, which is indicated by inserted lines (line AB and line CD). TEM images of sample C (c and c') and sample D (d and d'). Scale bar are (c) 20nm, (c') 5nm, (d) 20nm, and (d') 5nm.

XRD patterns of MnO_2 nanosheets

XRD patterns of sample A, B, C, and D are exhibited in Figure S4. It shows that all samples possess similar XRD profiles. All profiles are emerged with a few of broad peaks, which indicate that all samples present in an amorphous state.

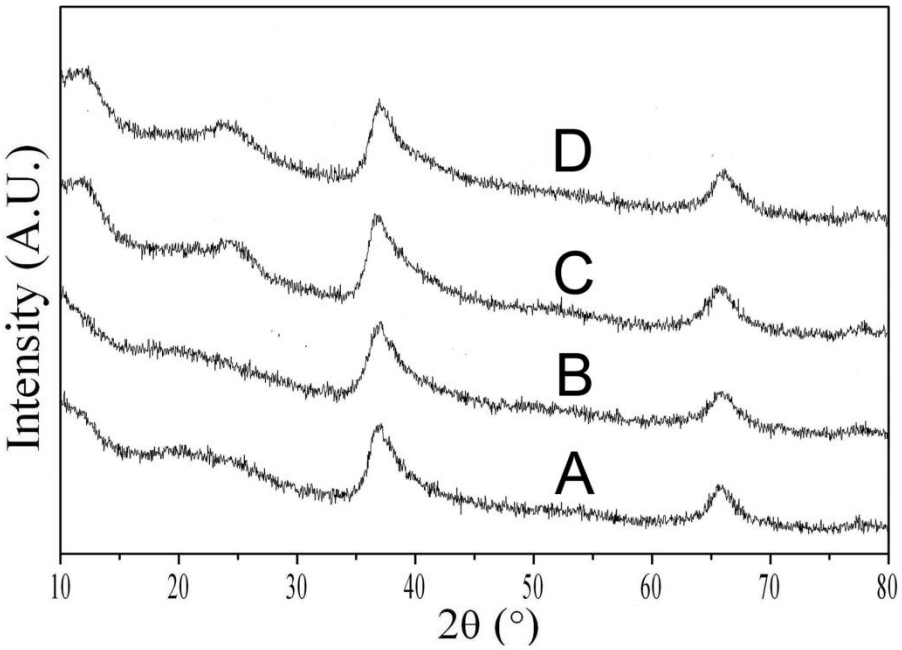

Fig. S4 XRD patterns of sample A, B, C and D

Raman spectra analysis of MnO_2 nanosheets

The Raman spectra of sample A, B, and D are shown in Figure S5. The spectrum of sample C is shown in Figure S7. It can be seen that all samples present in an amorphous state.

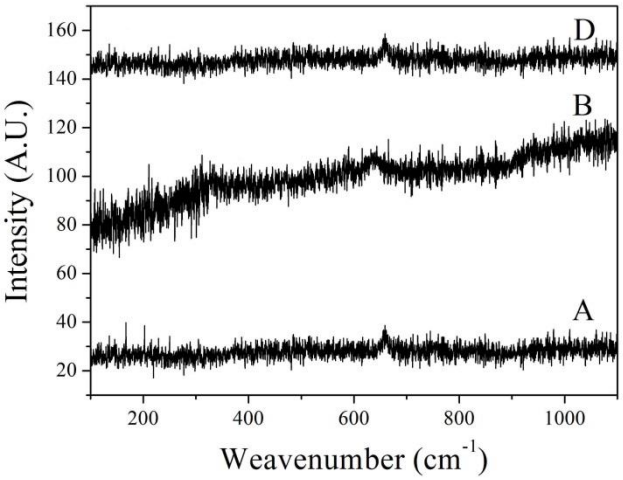

Fig. S5 Raman spectra of sample A, B, and D

XPS spectra analysis of MnO_2 nanosheets

The manganese average state for MnO_2 can be calculated from the signal of the Mn-O-Mn and Mn-OH components according to following equation:

$$\text{Average state} = (\text{Ⅳ}*(S_{\text{Mn-O-Mn}} - S_{\text{Mn—OH}}) + \text{Ⅲ}* S_{\text{Mn—OH}})/ S_{\text{Mn-O-Mn}} \quad (3)$$

Where *S* stands for signal of the different components of the O 1s spectra. Since all manganese atoms are bonded to an oxygen atom, the Mn-O-Mn signal should represent the contribution of two species : hydroxide MnOOH and oxide MnO_2. Hence, the XPS signal related to Mn(Ⅳ) species can be calculated by subtracting the contribution of hydroxyl group (MnOOH) from the Mn-O-Mn signal. Figure S4 shows the XPS spectra of Mn 2p and O 1s.

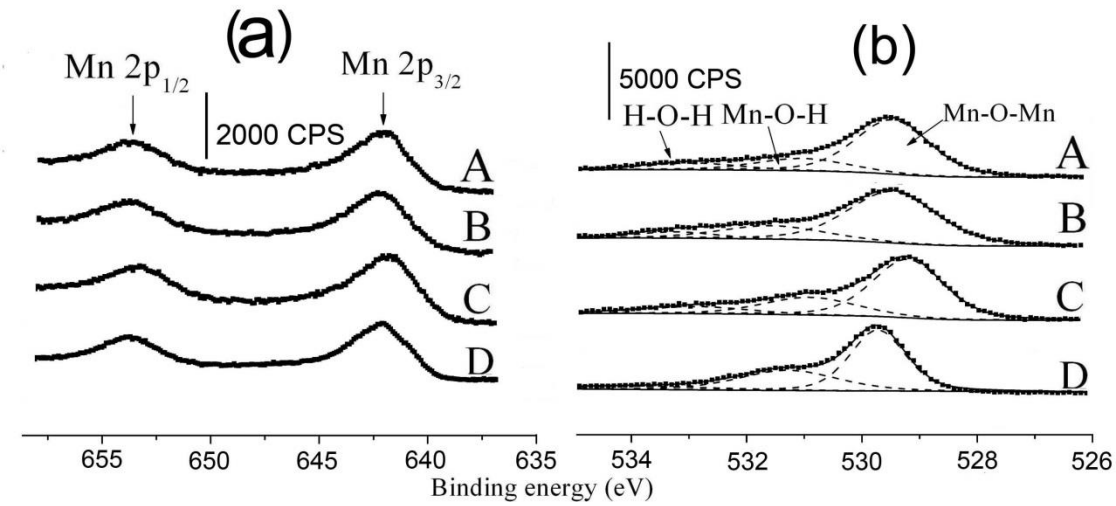

Fig. S6 XPS spectra of a) Mn 2p and b) O 1s

Table. S1 XPS peak analysis of MnO_2 samples. The deconvoluted data for the Mn $2p_{3/2}$ and O 1s spectra.

sample	Mn $2p_{3/2}$ BE (eV)[a]	O 1s			ΔBE_{Mn-O}[b] (eV)	Average state[c]
			Eb (eV)	Area %		
A	642.11	Mn-O-Mn	529.47	69.56	112.64	3.72
		Mn-OH	531.04	19.62		
		H-O-H	532.92	10.82		
B	642.04	Mn-O-Mn	529.46	68.11	112.58	3.71
		Mn-OH	531.22	20.04		
		H-O-H	533.01	11.85		
C	642.21	Mn-O-Mn	529.47	70.70	112.74	3.69
		Mn-OH	531.56	21.61		
		H-O-H	533.23	7.68		
D	641.79	Mn-O-Mn	529.20	63.49	112.59	3.64
		Mn-OH	530.90	25.21		
		H-O-H	532.87	11.30		

[a] Binding energies of peak position.
[b] The separation of peak position between Mn $2p_{3/2}$ and O 1s at the lowest position.
[c] The Mn mean state was obtained by the relative area calculation of the O 1s components.

CV plots of MnO_2 nanosheets

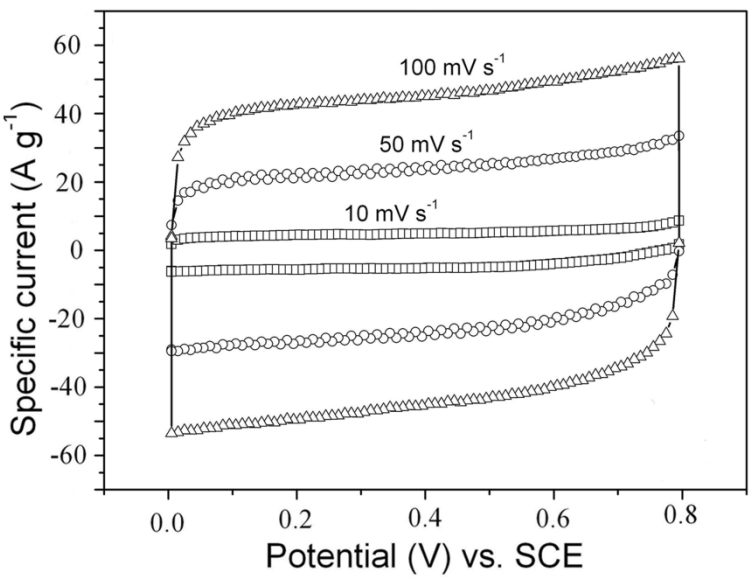

Fig. S7 CV plots of sample C at various sweep rates.

Cycle performance of MnO_2 nanosheets

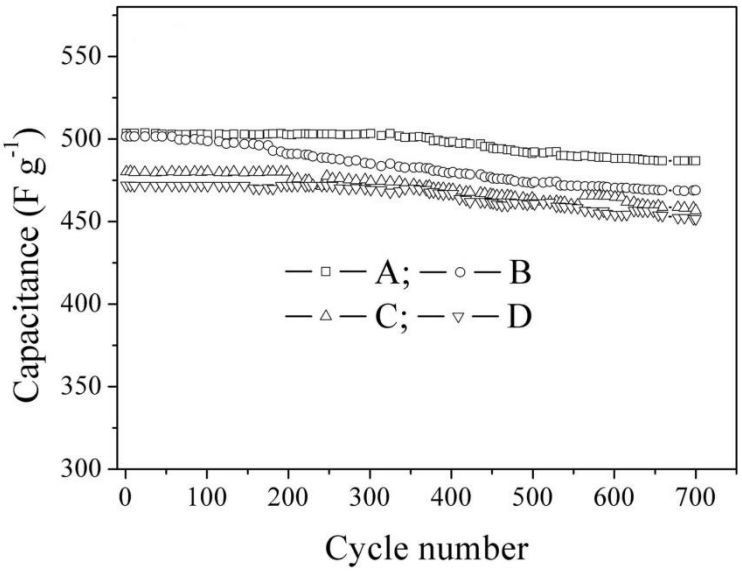

Fig. S8 Cycle performance of MnO_2 nanosheets

2. 0D sphere and 1D rod

XRD patterns of 0D sphere and 1D rod

XRD patterns of 0D MnO_2 sphere and 1D MnO_2 rod are exhibited in Figure S8. It shows that 0D sphere and 1D rod possess similar XRD profiles with 2D nanosheet. All profiles are emerged with a few of broad peaks, which indicate that all samples present in an amorphous state. 0D sphere and 1D rod MnO_2 samples possess similar crystalline structure with 0D sphere and 1D rod samples.

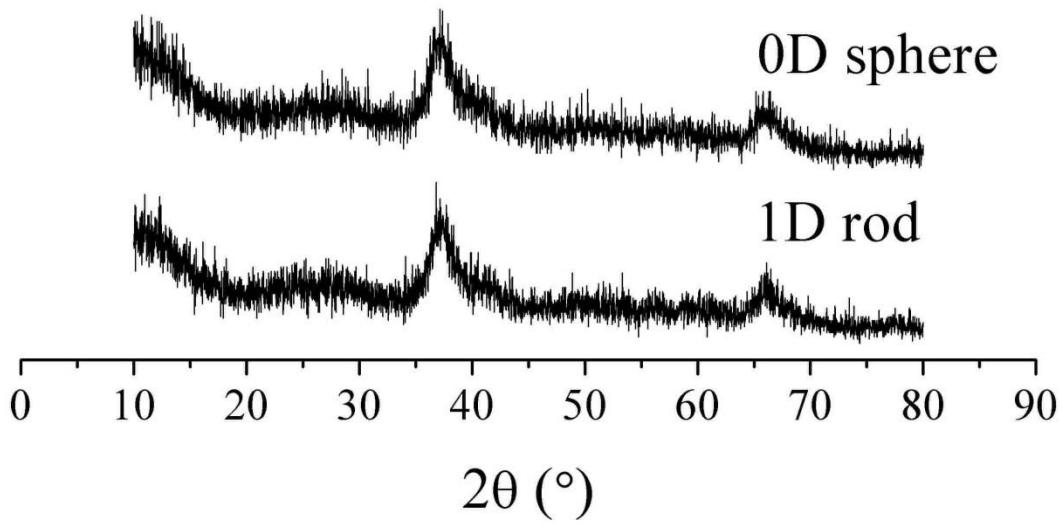

Fig. S9 XRD patterns of 0D sphere and 1D rod

SEM images of 0D MnO_2 sphere and 1D MnO_2 rod

The SEM images of 0D sphere are shown in Figure S10, which indicates that this MnO_2 sample exhibits a spherical shape with ~30 nm in diameter.

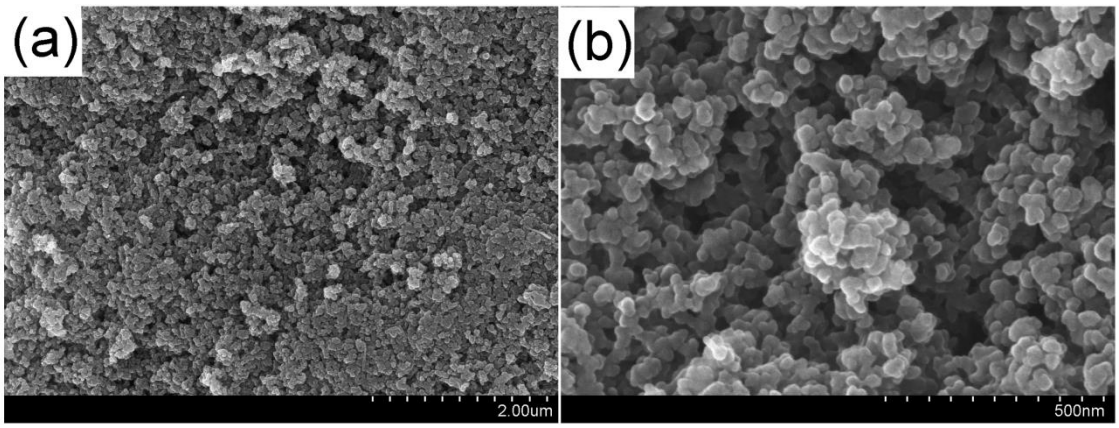

Fig. S10 SEM images of 0D MnO_2 sphere at low (a) and high (b) resolutions

The SEM images of 1D rod are shown in Figure S11, which indicates that this MnO_2 sample exhibits a rod shape with ~12 nm in diameter and ~100 nm in length.

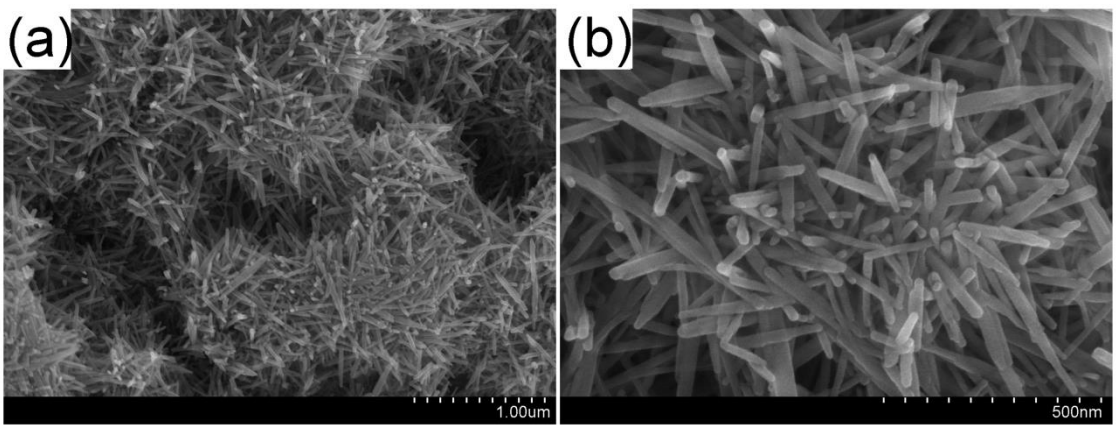

Fig. S11 SEM images of 1D MnO_2 rod at low (a) and high (b) resolutions

3. Samples of heat treated sample C

To further investigate the properties of MnO_2 sheet, sample C was annealed at 200, 300, 450 and 600 ℃ in air condition for 10 h, which are denoted as C-200, C-300, C-450, and C-600, respectively.

TEM images of sample C-300 (a1 and a2), C-450 (b1 and b2)

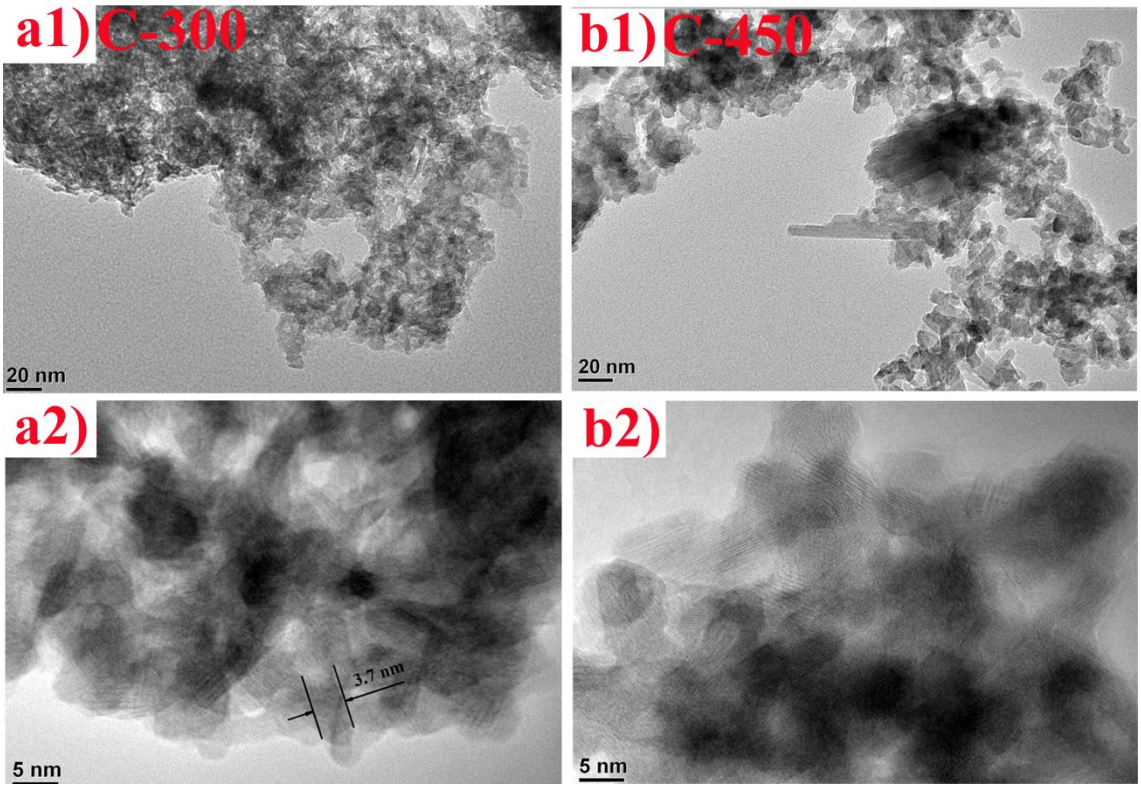

Fig. S12 TEM images of sample C-300 (a1 and a2), C-450 (b1 and b2).

TG and DSC curves of sample C

The thermogravimetric analysis (TG) and differential scanning calorimetry (DSC) curves of sample C show ca. 20% weight loss and endotherm around 100 ℃, which correspond to dehydration of the powders (Figure S13). Small weight loss and exotherm around 450 ℃ could attribute to the loss of oxygen from MnO_2 lattice resulting in phase transition from MnO_2 to Mn_2O_3.

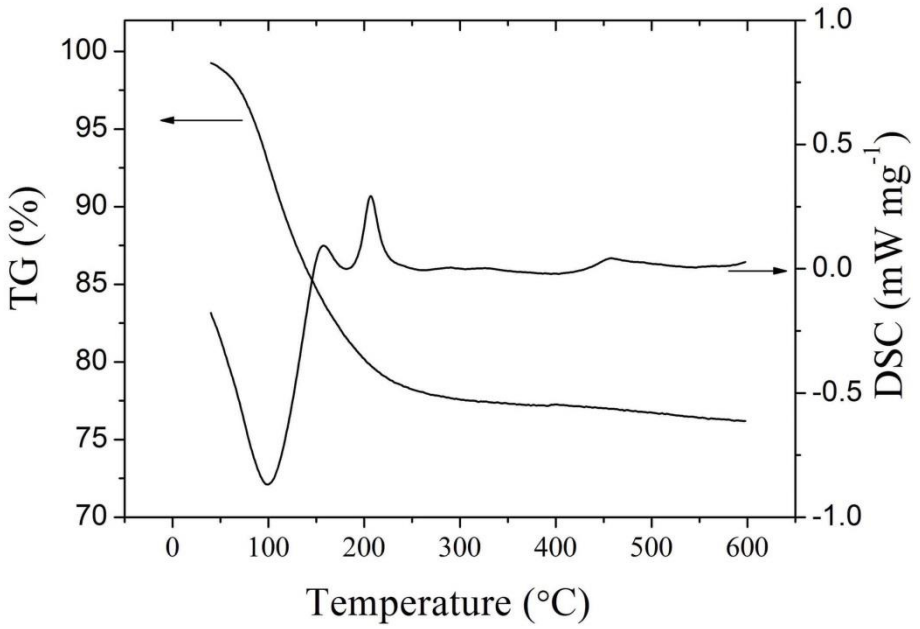

Fig. S13 TG and DSC curves of sample C

Raman spectra of sample C, C-200, C-300, C-450 and C-600

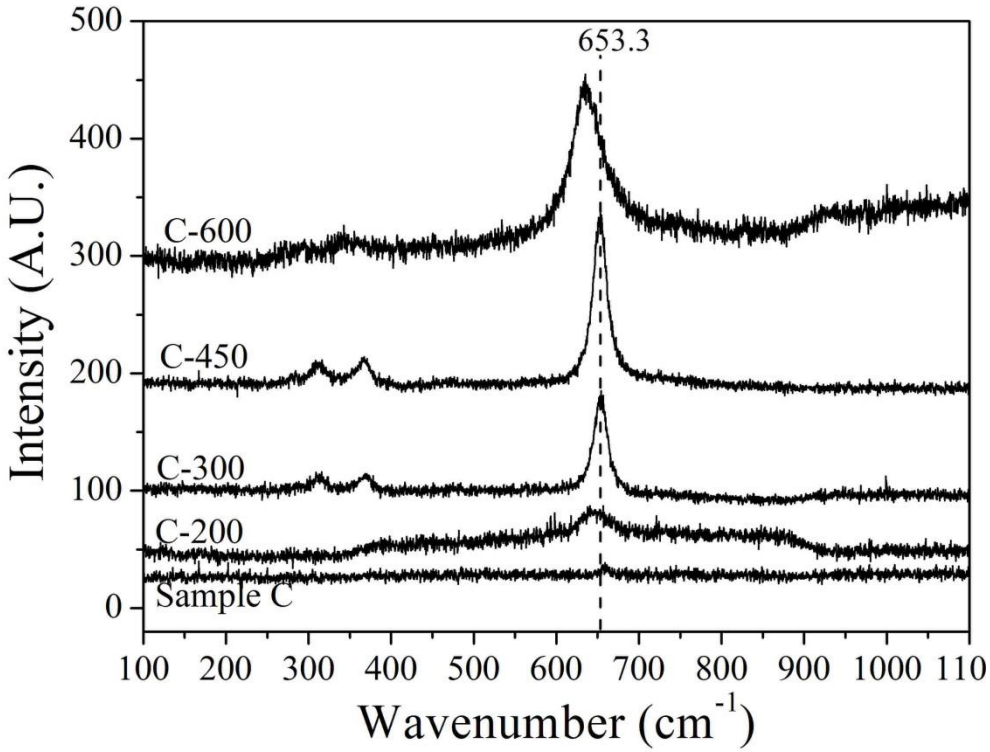

Fig. S14 Raman spectra of C, C-200, C-300, C-450 and C-600

CV plots of sample C-200, C-300, C-450 and C-600

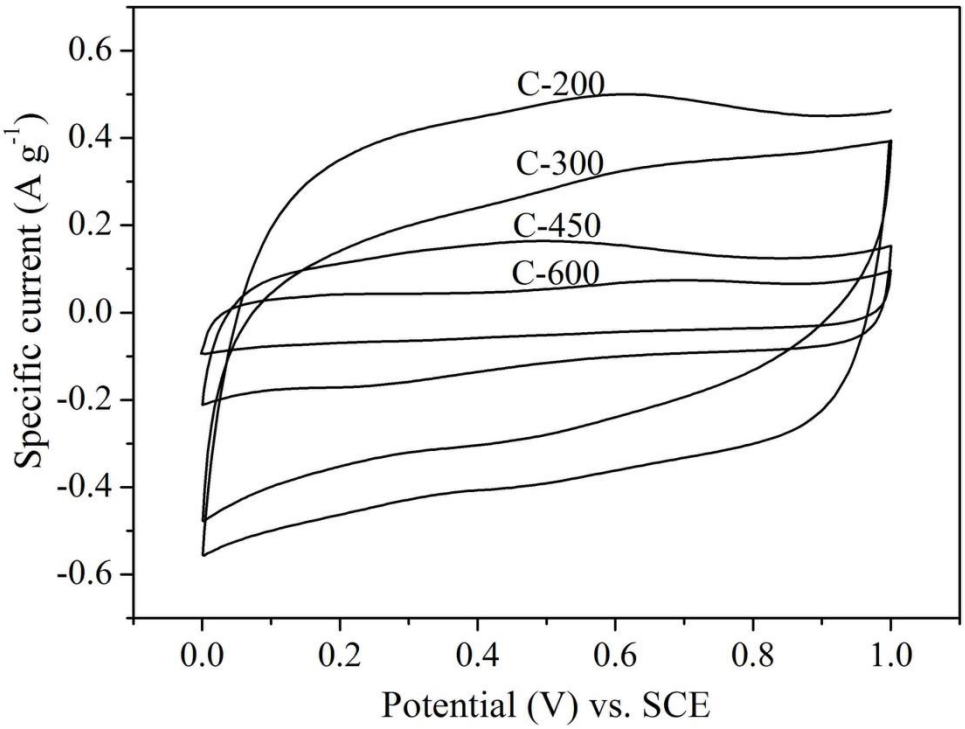

Fig. S15 CV plots of sample C-200, C-300, C-450 and C-600